

Mechanistic Study on Iron Solubility in Atmospheric Mineral Dust Aerosol: Roles of Titanium, Dissolved Oxygen, and Solar Flux in Solutions Containing Different Acid Anions

Eshani Hettiarachchi and Gayan Rubasinghe*

Department of Chemistry, New Mexico Institute of Mining and Technology, Socorro, NM, 87801

eshani.hettiarachchi@student.nmt.edu

*gayan.rubasinghe@nmt.edu

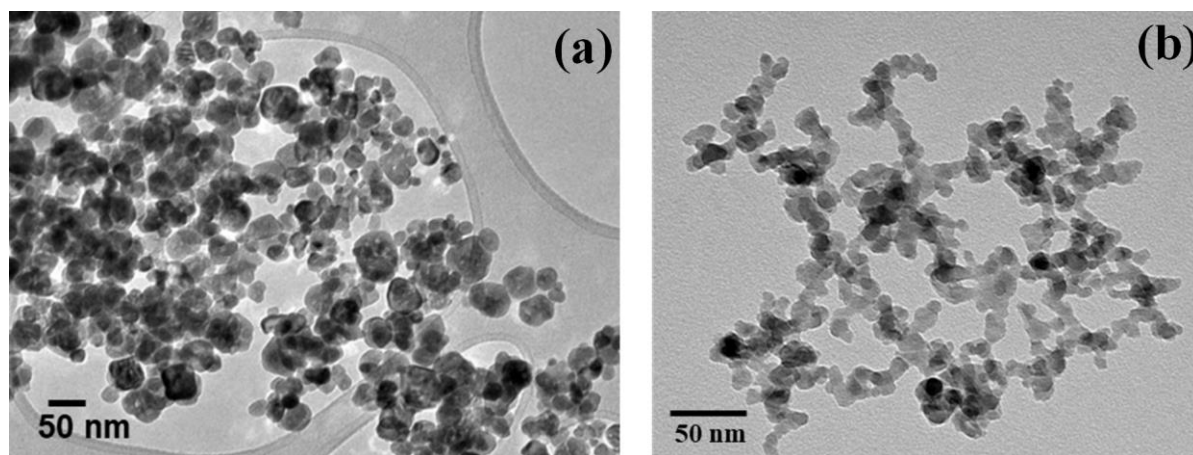


Figure S1: TEM images of (a) Hematite¹ (b) Anatase²

Table S1: The percentage of total Fe solubility

| System | % total Fe solubility | | | | | | | |
|------------------------------------|--------------------------|-----------------------|--------------------------|-----------------------|--------------------------|-----------------------|--------------------------|-----------------------|
| | Dark condition | | | | Light condition | | | |
| | deoxygenated | | oxygenated | | deoxygenated | | oxygenated | |
| | without TiO ₂ | with TiO ₂ | without TiO ₂ | with TiO ₂ | without TiO ₂ | with TiO ₂ | without TiO ₂ | with TiO ₂ |
| HCl | 1.46±0.11 | 0.37±0.9 | 1.08±0.03 | 0.78±0.07 | 0.83±0.04 | 1.20±0.05 | 1.25±0.01 | 1.79±0.01 |
| H ₂ SO ₄ | 1.71±0.16 | 0.69±0.11 | 0.79±0.05 | 0.75±0.07 | 1.23±0.01 | 2.74±0.11 | 1.61±0.03 | 2.63±0.20 |
| HNO ₃ | 0.68±0.02 | 0.83±0.04 | 2.65±0.08 | 1.92±0.06 | 0.85±0.01 | 1.19±0.03 | 1.14±0.04 | 1.41±0.07 |
| Controlled pH; HNO ₃ | 0.68±0.02 | 0.69±0.01 | -- | -- | -- | -- | -- | -- |
| IPA:HNO ₃ | -- | -- | -- | -- | 0.98±0.02 | 1.02±0.03 | -- | -- |

Fe Dissolution as a Function of Time in the Dark Deoxygenated/ N₂ Sparged Conditions

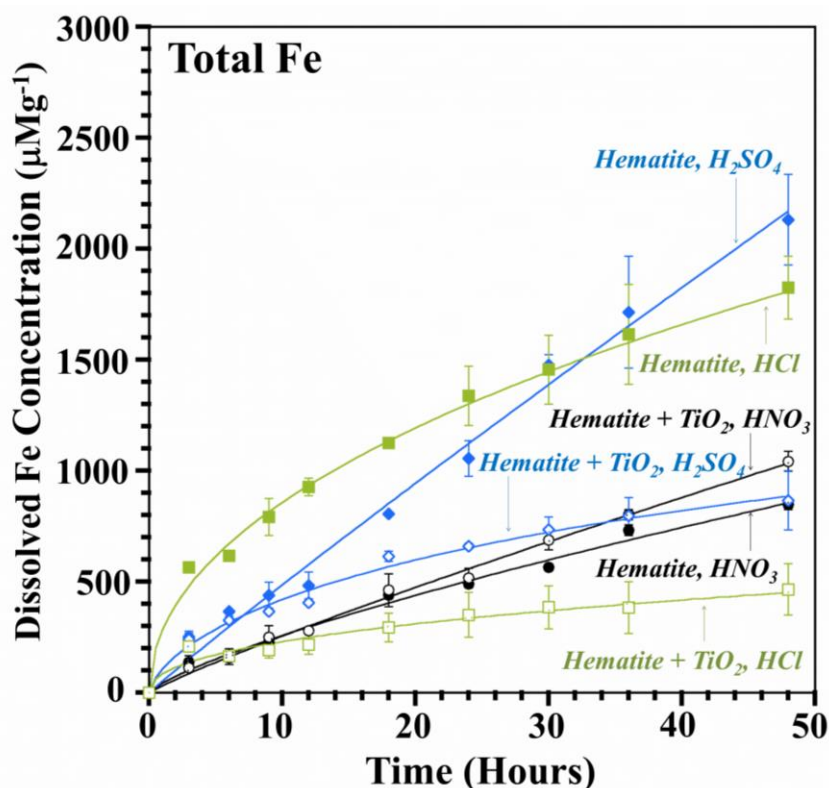


Figure S2: Total Fe dissolution from hematite and hematite with TiO₂ as a function of time in nitrate, sulfate and chloride in deoxygenated dark conditions with initial pH of 2. Open markers are hematite + TiO₂ and closed markers are hematite alone. Circles, HNO₃, squares, HCl, and diamonds, H₂SO₄. The data has fitted to Langmuir type model.

Fe Dissolution from hematite in the presence of amorphous titania – suggesting that the crystallinity of TiO₂ does not affect the Fe dissolution enhancement

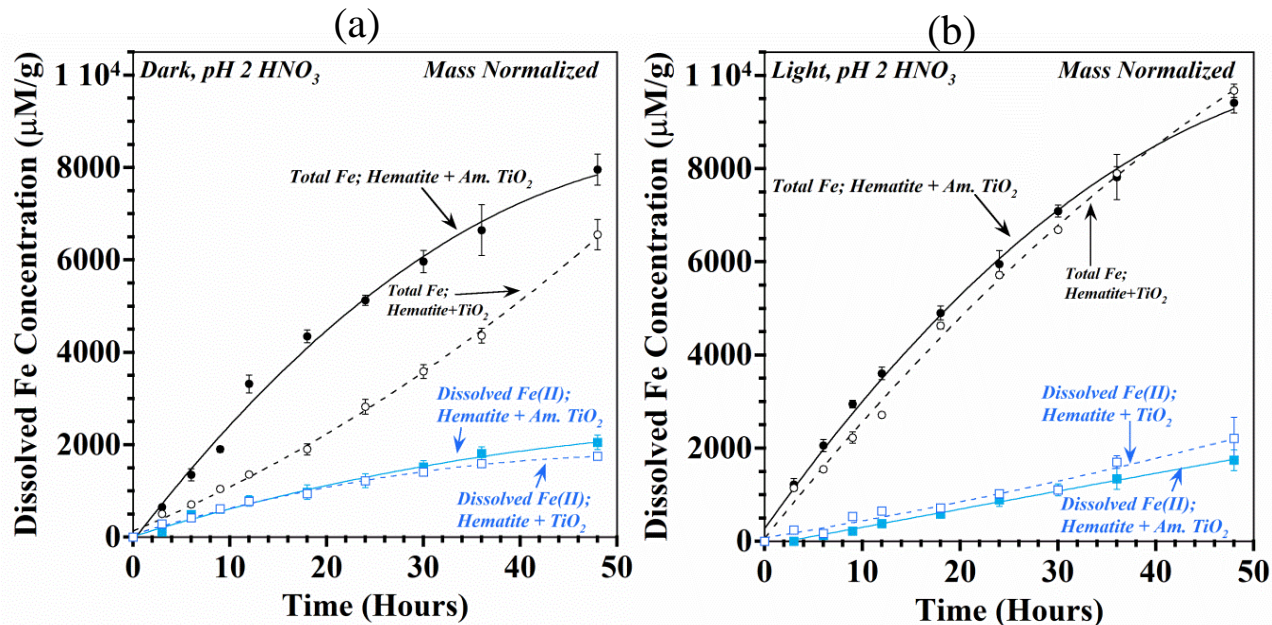
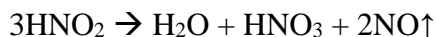
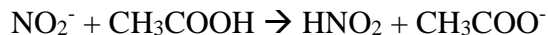


Figure S3: A comparison of the dissolved total Fe and Fe(II) concentrations from “hematite +amorphous titania mixture” and “hematite+TiO₂ mixture” in initial pH of pH 2 HNO₃, (a) dark (b) light. Data are fitted to Langmuir-type model.³

Nitrite Assay Test⁴

The nitrite was detected using mild condition brown ring test. First, A 25% Fe(II) sulfate solution acidified with acetic acid was prepared. The nitrite solution was added slowly to this freshly prepared Fe(II) sulfate solution and the formation of a brown ring in the interface was observed. Controlled tests were conducted for sodium nitrite and for sodium nitrite plus sodium nitrate mixtures. Another negative control was conducted with sodium nitrate for which no brown ring formation was observed.

Reactions:



[Fe₂NO]SO₄ is responsible for the brown coloration.

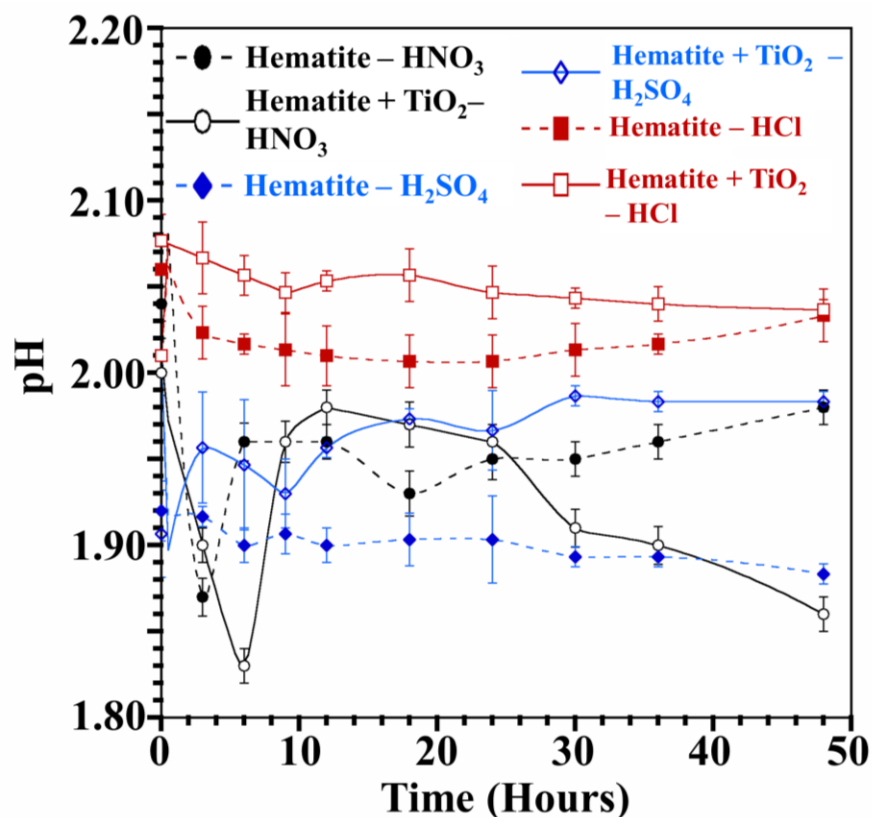
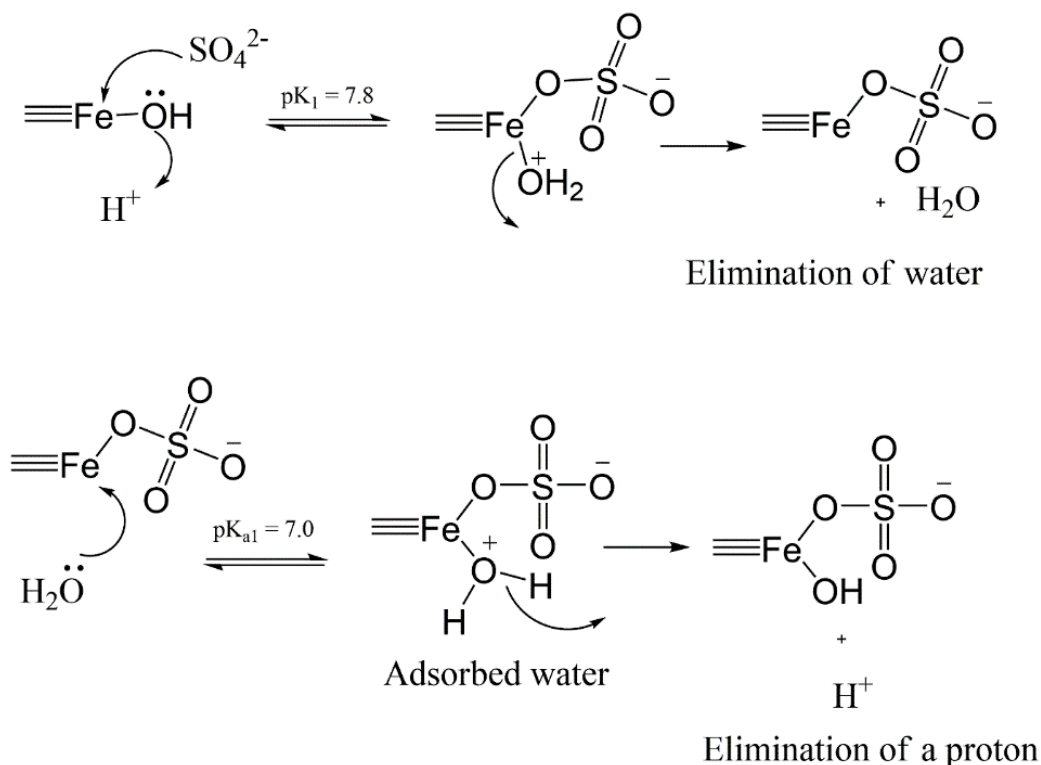


Figure S4: pH of the medium as a function of time for hematite and hematite with TiO₂ systems in nitrate, sulfate and chloride systems in dark deoxygenated conditions.

Table S2: Post pH Assessment of the Experiments

| System | ΔpH (pH of 48 th hr – initial pH) | | | | | | | |
|--------------------------------|--|-----------------------|--------------------------|-----------------------|--------------------------|-----------------------|--------------------------|-----------------------|
| | Dark condition | | | | Light condition | | | |
| | deoxygenated | | oxygenated | | deoxygenated | | oxygenated | |
| | Without TiO ₂ | with TiO ₂ | without TiO ₂ | with TiO ₂ | without TiO ₂ | with TiO ₂ | without TiO ₂ | with TiO ₂ |
| HCl | 0.02 | 0.03 | 0.08 | 0.13 | 0.08 | 0.005 | 0.03 | 0.005 |
| H ₂ SO ₄ | -0.13 | -0.03 | -0.07 | -0.02 | -0.025 | -0.09 | -0.02 | -0.004 |
| HNO ₃ | 0.03 | -0.15 | 0.04 | 0.02 | -0.01 | -0.05 | 0.04 | 0.09 |

pH variation in the sulfate medium



Scheme 1: A possible mechanism for the adsorption of sulfate on hematite surface allowing an overall decrease of pH of the medium. pK_1 and pK_{a1} were adopted from Blesa et al, 2000.⁵

As proton-promoted mechanisms consume protons, an increase of pH is expected as the reaction progresses.⁶⁻⁸ However, contrary to this, the pH was slightly decreased for H_2SO_4 (**Table S2**). Adsorption of oxyanions with multiple negative charges can either eliminate surface hydroxyl groups or exchange protons of proximal adsorbed water molecules, releasing protons to the medium.^{5,9-11} Thus, the observed lowering of pH for sulfate can be attributed to the possibility of establishing such an equilibrium as illustrated in **Scheme 1**. Here, the release of protons (H^+) by dissociation of adsorbed water may also regenerate the surface hydroxyl groups.^{5,11} These low pH conditions can further enhance iron dissolution in the presence of sulfate as the proton-promoted dissolution becomes more favorable.

Iron Dissolution under Oxidizing Environment

Dissolved oxygen can impact on mineral dissolution due to its capacity to change mobility and chemical speciation of dissolved metals. In order to study the impact of dissolved oxygen on hematite dissolution, experiments were conducted in media sparged with O₂.

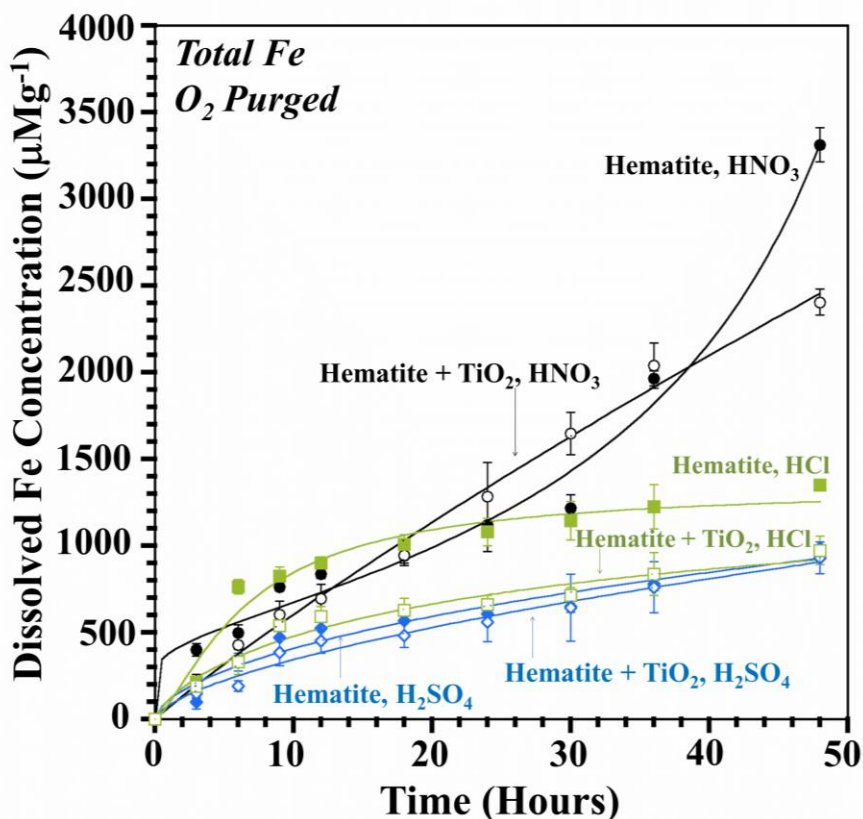
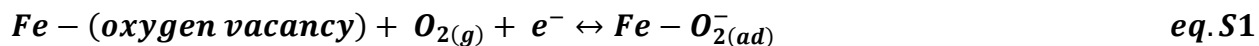


Figure S5: The total Fe dissolution as a function of time in the presence of dissolved oxygen under dark conditions. Open markers are hematite + TiO₂ and closed markers are hematite alone. Circles, HNO₃, squares, HCl, and diamonds, H₂SO₄. The data has fitted to Langmuir type model.

Role of Acid Anion in an Oxidizing Deliquescence Layer

Figure S5 shows total Fe dissolution from hematite with and without TiO₂ in the presence of HNO₃, H₂SO₄ and HCl in an oxidizing environment under dark conditions. The dissolution of hematite was highest in the presence of HNO₃ followed by HCl and H₂SO₄ as opposed to deoxygenated conditions where the highest dissolution was observed in H₂SO₄ while the lowest was in the presence of HNO₃. The initial rates of Fe dissolution were 52 ± 3 , 32 ± 1 and 56 ± 3 $\mu\text{M g}^{-1} \text{ hr}^{-1}$ for HNO₃, H₂SO₄ and HCl, respectively. When compared to their respective extent of Fe dissolutions under deoxygenated conditions, hematite dissolved at least 4-fold more under oxidizing conditions in the presence of HNO₃ whereas the Fe dissolution was diminished 2.2-fold and 1.4-fold in the presence of H₂SO₄ and HCl, respectively.

Under oxic conditions, as the redox potential (E_h) of the system is lower, the tendency for iron minerals to reprecipitate is higher.¹² In H_2SO_4 solutions, hematite as well as ferric sulfate hydrates can precipitate thereby passivating the active sites on the surface. This can lead to lowering in extent of Fe dissolution compared to deoxygenated conditions. In the presence of Cl^- anion, the low Fe dissolution could be due to the formation of minerals such as goethite, which demonstrated a limited dissolution capacity in HCl solutions.^{8,13} Similarly, the observed high solubility in HNO_3 could be due to the high dissolution capacity of these precipitating minerals, i.e. high goethite dissolution in HNO_3 solutions. The XRD pattern of acid-processed hematite under HNO_3 and water vapor confirms the formation of 17% goethite (**Figure S6**). Formation of these minerals was not observed under deoxygenated conditions due to their lower tendency to precipitate in less aerated aqueous solutions.¹⁴ On the other hand, the reactivity of ferric oxide surfaces become more complex in the presence of oxygen. Hematite is well known to present oxygen vacancies where the number of vacancies depends on the environmental conditions such as humidity.^{11,15,16} Further, these vacancies can react with dissolved oxygen, as shown in **equations S1** and **S2**, making the oxide surface more reactive to redox chemistry.^{11,15}



Where e^- is an electron trapped in the oxygen vacancy, ~ 0.75 eV below the conduction band of hematite.¹⁵ The generated $Fe-2O_{(ad)}^-$ species is a potential electron acceptor. Nitrate can show strong redox activity both in aqueous and adsorbed phases. Therefore, it is possible that nitrate is involved in the surface chemistry on hematite surfaces in the presence of dissolved oxygen. However, further research is needed to understand the dissolution of hydrated hematite in the presence of dissolved oxygen by various environmentally relevant anions such as nitrate.

Role of TiO_2 in Oxic Environments during Nighttime

The extent of total Fe dissolution in hematite mixed with TiO_2 under oxic conditions was lower than that of only hematite (**Figure S6**). Hematite mixed with TiO_2 dissolved at least 1.4-fold less in the presence of HNO_3 and HCl, and slightly lower (~ 1.1 -fold) in H_2SO_4 than their respective systems containing only hematite. The competition among different mineral surfaces for acid anions, similar to that in deoxygenated conditions, could cause the observed low Fe dissolution. However, a redox cycling between minerals and the adsorbed nitrate may not be prominent under oxic environments, unlike the anoxic conditions; hence all three anions tested demonstrated a decrease of the dissolved total Fe concentration.

In a deliquescence layer rich with dissolved oxygen, the $Fe(II)$ formation was not observed for any of the six systems. For the HNO_3 system, nitrite formation was tested and found not to occur. The post pH assessment suggests the slight decrease only for H_2SO_4 systems. (**Table S2**)

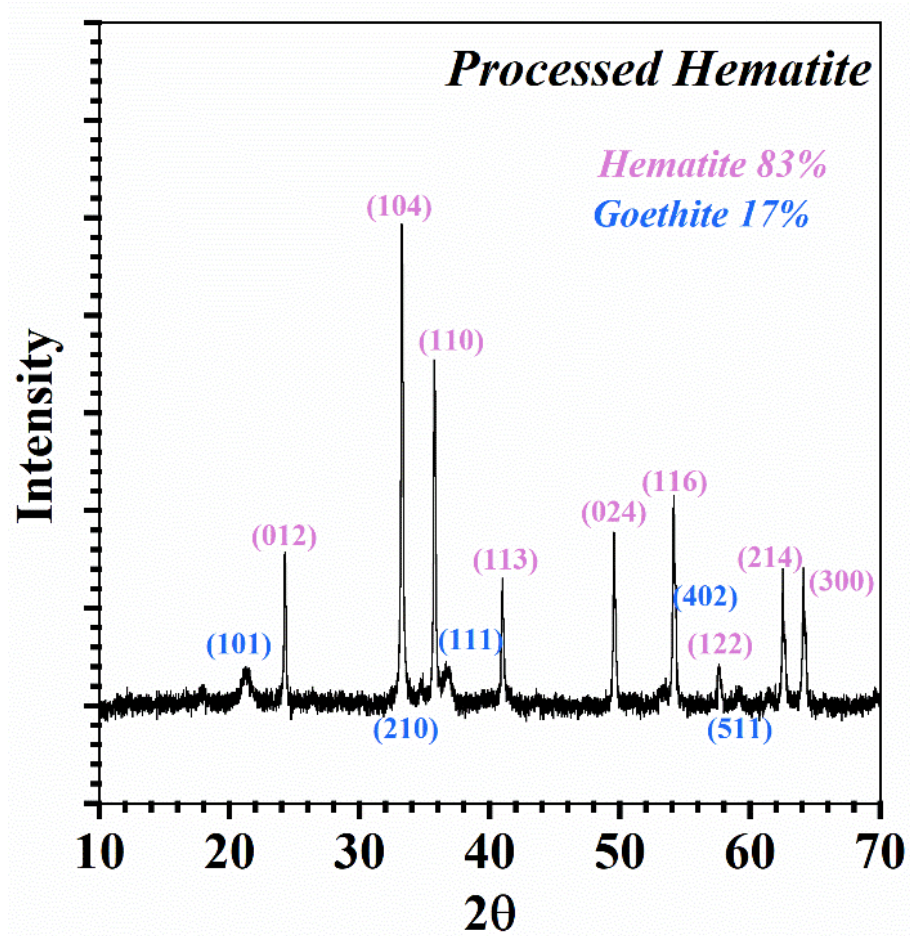


Figure S6: XRD image of pure hematite exposed to gaseous HNO_3 for 48 hours in the humid conditions

Dissolved Fe Concentration as a function of Time in the Simulated Sunlight

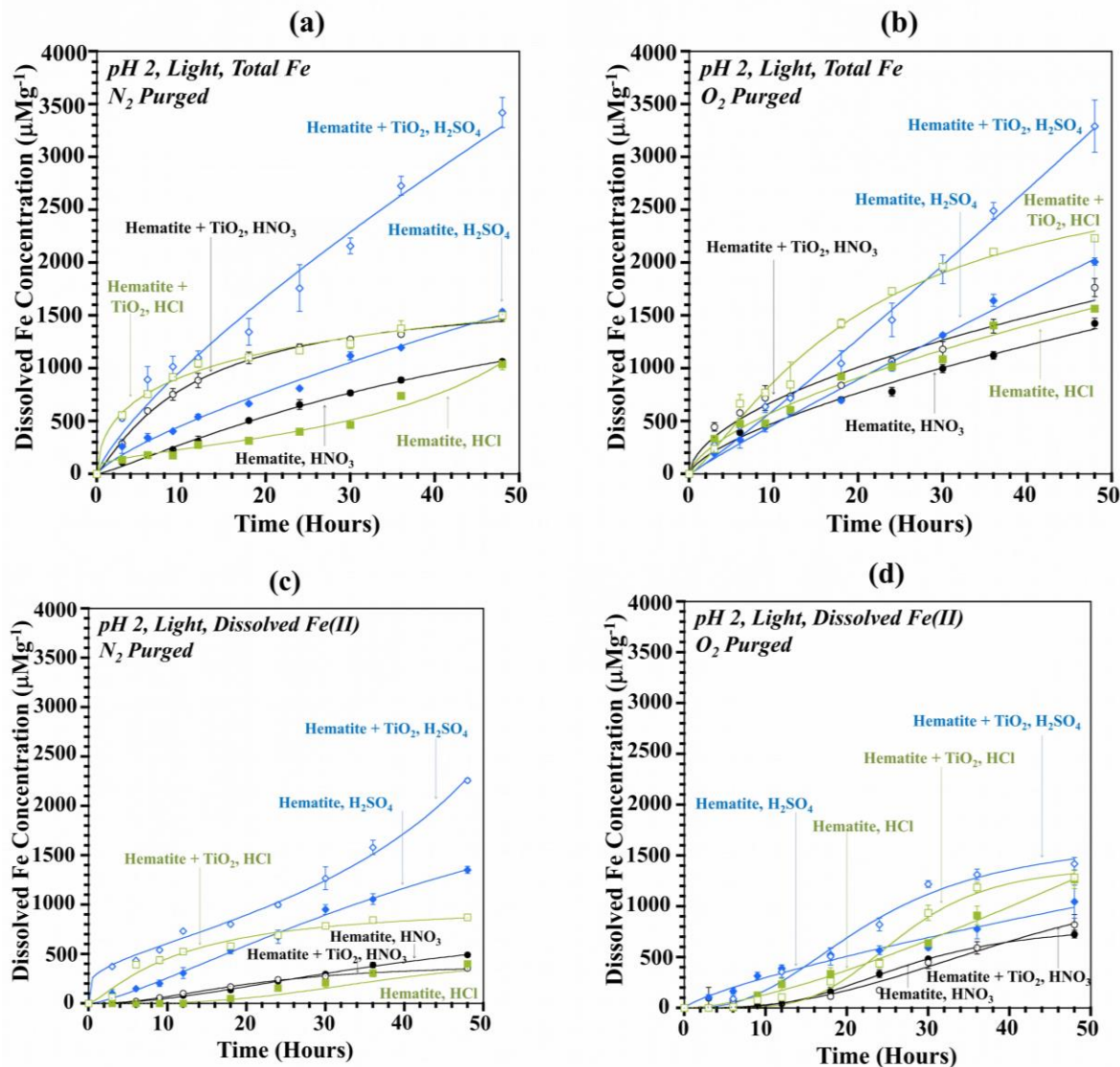


Figure S7: The total Fe dissolution from hematite as a function of time in the presence of simulated sunlight. The total dissolved Fe in (a) anoxic conditions (b) oxic conditions, and dissolved Fe(II) in (c) anoxic conditions (d) oxic conditions. Open markers are hematite + TiO_2 and closed markers are hematite alone. Circles, HNO_3 , squares, HCl , and diamonds, H_2SO_4 . The data has fitted to Langmuir type model.

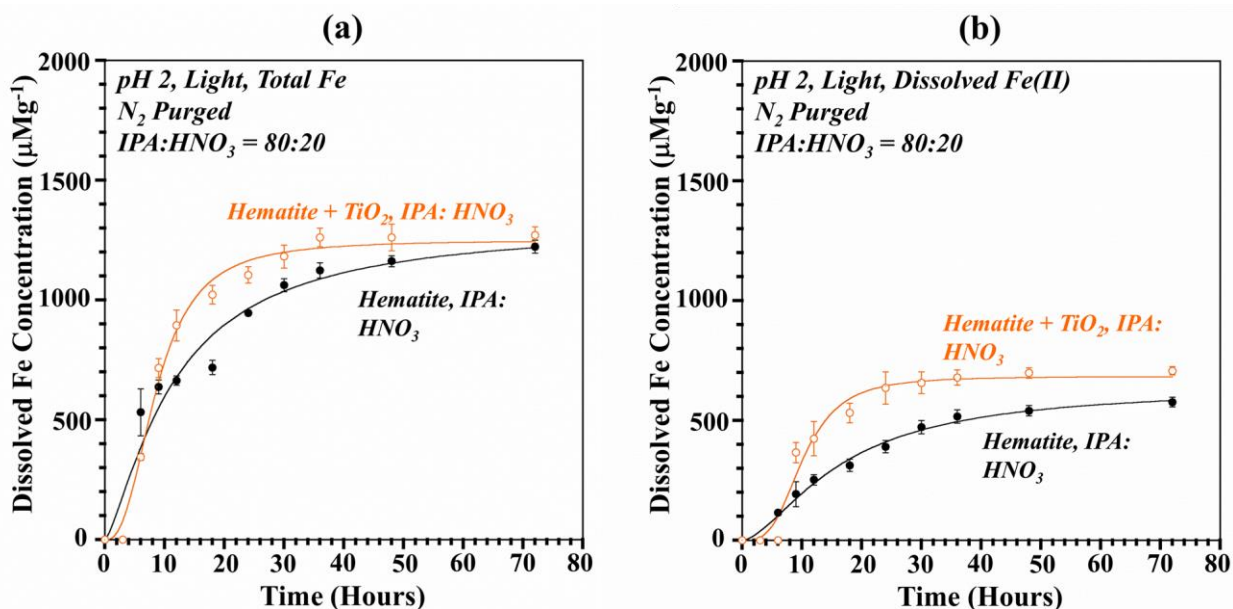


Figure S8: The dissolved Fe from hematite alone and hematite with TiO₂ in IPA:HNO₃ medium as a function of time. (a) total dissolved Fe, (b) Dissolved Fe(II). Open circles are for hematite with TiO₂ and closed circles are hematite alone. Data are fitted to Langmuir type model.

- (1) Hettiarachchi, E.; Hurab, O.; Rubasinghege, G. Atmospheric Processing and Iron Mobilization of Ilmenite: Iron-Containing Ternary Oxide in Mineral Dust Aerosol. *J. Phys. Chem. A* **2018**, *122*, 1291–1302. <https://doi.org/10.1021/acs.jpca.7b11320>.
- (2) Hettiarachchi, E.; Reynolds, R. L.; Goldstein, H. L.; Moskowitz, B.; Rubasinghege, G. Iron Dissolution and Speciation in Atmospheric Mineral Dust: Metal-Metal Synergistic and Antagonistic Effects. *Atmos. Environ.* **2018**, *187*, 417–423. <https://doi.org/10.1016/j.atmosenv.2018.06.010>.
- (3) Hettiarachchi, E.; Reynolds, R. L.; Goldstein, H. L.; Moskowitz, B.; Rubasinghege, G. Bioavailable Iron Production in Airborne Mineral Dust: Controls by Chemical Composition and Solar Flux. *Atmos. Environ.* **2019**, *205*, 90–102. <https://doi.org/10.1016/j.atmosenv.2019.02.037>.
- (4) Svehla, G. *Vogel's Textbook Of Macro And SemiMicro Qualitative Inorganic Analysis*, 5th ed.; Longman Group Limited: London and New York, 1979.
- (5) Blesa, M. A.; Weisz, A. D.; Morando, P. J.; Salfity, J. A.; Magaz, G. E.; Regazzoni, A. E. The Interaction of Metal Oxide Surfaces with Complexing Agents Dissolved in Water. *Coord. Chem. Rev.* **2000**, *196* (1), 31–63. [https://doi.org/10.1016/S0010-8545\(99\)00005-3](https://doi.org/10.1016/S0010-8545(99)00005-3).
- (6) Parfitt, G. D. Surface Chemistry of Oxides. *Pure Appl. Chem.* **1976**, *48* (4), 415–418.
- (7) Wiederhold, J. G.; Kraemer, S. M.; Teutsch, N.; Borer, P. M.; Halliday, A. N.; Kretzschmar, R. Iron Isotope Fractionation during Proton-Promoted, Ligand-Controlled, and Reductive Dissolution of Goethite. *Environ. Sci. Technol.* **2006**, *40*, 3787–3793.

<https://doi.org/10.1021/es052228y>.

- (8) Rubasinghege, G.; Lentz, R. W.; Scherer, M. M.; Grassian, V. H. Simulated Atmospheric Processing of Iron Oxyhydroxide Minerals at Low PH: Roles of Particle Size and Acid Anion in Iron Dissolution. *Proc. Natl. Acad. Sci.* **2010**, *107*, 6628–6633. <https://doi.org/10.1073/pnas.0910809107>.
- (9) Al-Abadleh, H. A.; Al-Hosney, H. A.; Grassian, V. H. Oxide and Carbonate Surfaces as Environmental Interfaces: The Importance of Water in Surface Composition and Surface Reactivity. *J. Mol. Catal. A Chem.* **2005**, *228* (1–2), 47–54. <https://doi.org/10.1016/j.molcata.2004.09.059>.
- (10) Bordiga, S.; Groppo, E.; Agostini, G.; van Bokhoven, J. A.; Lamberti, C. Reactivity of Surface Species in Heterogeneous Catalysts Probed by In Situ X-Ray Absorption Techniques. *Chem. Rev.* **2013**, *113* (3), 1736–1850. <https://doi.org/10.1021/cr2000898>.
- (11) Grassian, V. H. Surface Science of Complex Environmental Interfaces: Oxide and Carbonate Surfaces in Dynamic Equilibrium with Water Vapor. *Surf. Sci.* **2008**, *602*, 2955–2962. <https://doi.org/10.1016/j.susc.2008.07.039>.
- (12) Brezonik, P.; Arnold, W. *Water Chemistry An Introduction to the Chemistry of Natural and Engineered Aquatic Systems*, 1st ed.; Oxford University Press: New York, 2011. <https://doi.org/978-0-19-973072-8>.
- (13) Riveros, P. A.; Dutrizac, J. E. The Precipitation of Hematite from Ferric Chloride Media. *Hydrometallurgy* **1997**, *46* (1–2), 85–104. [https://doi.org/10.1016/S0304-386X\(97\)00003-0](https://doi.org/10.1016/S0304-386X(97)00003-0).
- (14) Wehrli, B. Redox Reactions of Metal Ions at Mineral Surfaces. In *Aquatic Chemical Kinetics—Reaction Rates of Processes in Natural Waters*; Stumm, W., Ed.; Wiley-Interscience: New York, 1990; pp 311–335.
- (15) Lilley, C. M. The Role of Technology in Managing People Who Have Been Convicted of Internet Child Abuse Image Offences. *Child Abus. Rev.* **2016**, *25* (5), 386–398. <https://doi.org/10.1002/car.2444>.
- (16) Toledano, D. S.; Henrich, V. E. Kinetics of SO₂ adsorption on Photoexcited α -Fe₂O₃. *J. Phys. Chem. B* **2001**, *105*, 3872–3877. <https://doi.org/10.1021/jp003327v>.